View metadata, citation and similar papers at core.ac.uk

brought to you by CORE

provided by Heriot Watt Pure

Heriot-Watt University

Heriot-Watt University
Research Gateway

An impedance approach to reduce the contact-instability whilst drilling with active heave compensation

Hatleskog, Jan; Dunnigan, Mathew Walter

Published in:
Ocean Engineering

DOI:
10.1016/j.oceaneng.2012.04.001

Publication date:
2012

Link to publication in Heriot-Watt Research Gateway

Citation for published version (APA):
Hatleskog, J., & Dunnigan, M. W. (2012). An impedance approach to reduce the contact-instability whilst drilling with active heave compensation. Ocean Engineering, 49(n/a), 25-32. 10.1016/j.oceaneng.2012.04.001

Ocean Engineering 49 (2012) 25–32

Contents lists available at SciVerse ScienceDirect

Ocean Engineering

journal homepage: www.elsevier.com/locate/oceaneng

An impedance approach to reduce the contact-instability whilst drilling with active heave compensation

Jan T. Hatleskog, Matthew W. Dunnigan *

Department of Electrical, Electronics, and Computer Engineering, School of Engineering and Physical Sciences, Heriot-Watt University, Edinburgh, Scotland, EH14 4AS, UK

ARTICLE INFO

Article history:
Received 1 March 2011
Accepted 7 April 2012
Available online 3 May 2012

Keywords:
Active heave compensation
Impedance
Drilling
Contact-instability

ABSTRACT

The bit-bounce, or contact-instability, phenomenon which occurs in the drill string suspended from a floating vessel with an active drill string compensator to maintain a steady weight on the drill bit is investigated. This effect is sometimes ascribed to torsion effects when turning the drill bit, however, in this paper only the vertical effects induced by vessel heave are considered. A dynamic model is generated which is used for a set of simulations illustrating the contact-instability. An impedance approach for resolving this problem is described and included in the simulations which demonstrate that by modifying the impedance the bit-bounce is greatly reduced.

© 2012 Elsevier Ltd. All rights reserved.

1. Introduction

A floating vessel is subject to wind and wave disturbances and the resulting heave will affect the efficiency of the drilling process as the drill bit could be lifted clear of the bottom as the vessel heaves up and subsequently forced down very hard against the formation when heaving down. In order to mitigate the effect of this heave disturbance on the drilling performance a passive drill string compensator was introduced; it acts as a very low rate spring enabling the drill bit to maintain contact in moderate heave conditions (Bennett, 1997; Hatleskog, 1983; Woodall-Mason and Tilbe, 1976). The measure of compensator performance is the load variation which is kept relatively low so as not to adversely affect the drilling process, be it the rate of progress or the life of the drill bit. The active sub-system was added in the early 90's to improve the compensation performance, initially to extend the weather window for landing operations but has subsequently been used to improve the load variation whilst drilling. This simulation is based on the NOV Shaffer ACMC which is one of the main suppliers in this field.

However, even with active and passive heave compensation, a disturbance commonly referred to as bit-bounce or contact-instability may occur in some instances depending on the compensator and the bottom formation. Whereas the bit-bounce may sometimes be ascribed to a range of different torsion effects in the drill string, this paper specifically considers any vertically induced disturbances introduced by the compensator without the drill string being rotated. The objective of this paper is to show that the impedance approach may be used to remove, or minimise, this bit-bounce effect using an active heave compensator.

The paper briefly describes the drill string and compensator with an active sub-system in Sections 2 and 3. A dynamic model of the system is presented in Sections 4 and 5 which illustrates the contact-instability problem through a set of simulation results. Sections 6 and 7 present an impedance approach which may be used to deal with contact-instability and is incorporated in the dynamic model and simulation.

2. The crown Mounted drill string compensator system

The normal drill pipe is a tubular pipe with threaded pin box ends and is typically 9.65 m long with an outer diameter of 140 mm and an internal diameter of 100 mm. Three lengths of drill pipe are made up into 29 m lengths referred to as a stand, each stand being lowered into the well. However, the full drill string typically comprises three major elements; the bottom-hole assembly (BHA) which is made up of the drill bit doing the actual cutting and the drill collar comprising one, or more, larger diameter drill pipes to add weight onto the drill bit. Next follows a section of heavy weight drill pipe (HWDP) to provide a transition to the drill pipe which makes up most of the drill string length.

As the well will vary considerably in depth as the drilling progresses, the weight of the total drill string will vary greatly from the beginning of a well until it is completed and depends on the sea depth.

The drill string load is suspended from the crown block which is carried by two compensating cylinders with a stroke of 7.6 m and is supported by compressed air acting on the two pistons connected to a much larger air bank through a stand pipe and can support loads up to 450 t as illustrated in Fig. 1. The air bank volume is large compared to the compensator cylinder volume forming a low-rate spring in order to reduce the pressure

* Corresponding author. Tel.: +44 131 451 3346; fax: +44 131 451 4155.
E-mail address: m.w.dunnigan@hw.ac.uk (M.W. Dunnigan).

0029-8018/$ - see front matter © 2012 Elsevier Ltd. All rights reserved.
http://dx.doi.org/10.1016/j.oceaneng.2012.04.001

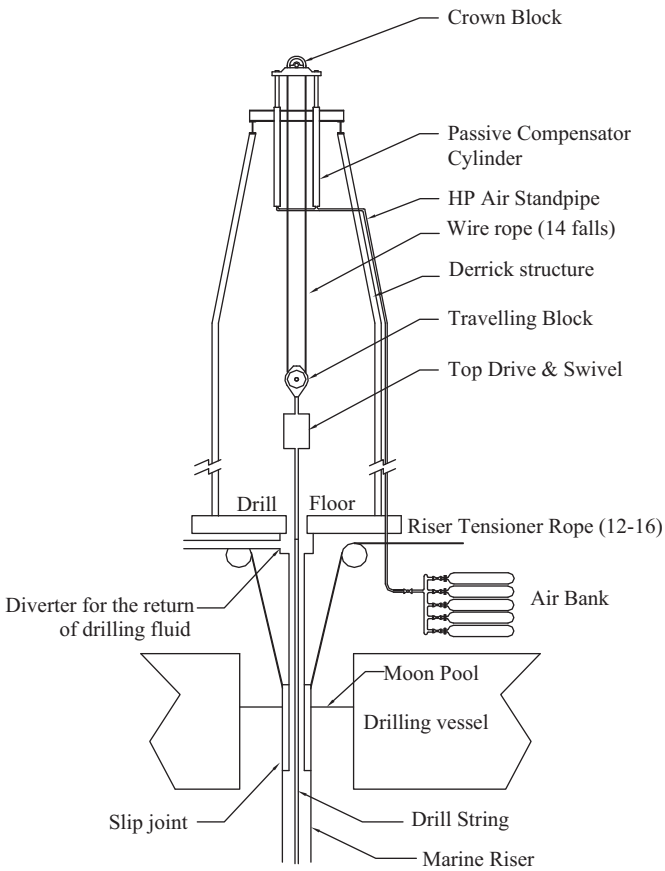

Fig. 1. The Crown Mounted Drill String Compensator (CMC). Located in the derrick crown and supporting the crown block.

variation due to changes in cylinder volume due to vessel heave (Hatleskog and Dunnigan, 2007a,b).

During drilling the air pressure is adjusted carrying most of the weight of the drill string but leaving a small portion to be carried by the drill bit acting on the bottom formation. As the vessel heaves upwards the air is compressed increasing the pressure and the weight on the drill bit reduces correspondingly; conversely the air volume expands to a lower pressure as the vessel heaves downwards and puts more weight onto the drill bit. The change in air volume is a function of heave resulting in a corresponding change in air pressure which is directly related to the total volumetric change in the compensator air sub-system.

In addition to the load variation due to air volume changes, there are two forms of friction due to compensator stroking. The compensator has a set of seals and bearing surfaces with the inevitable coulomb friction; in addition high pressure (HP) air is displaced from the compensator cylinders to the air bank which is made up of a set of air pressure vessels (APV's) through a long stand pipe and then back again as the vessel heaves up and down. This flow gives rise to pressure drops which results in viscous friction. Over the years a great deal of effort has been applied to minimise the compensator load variation within practical constraints. Whilst the seal friction has been improved having regard to the seal life, this means that a certain amount of stick-slip friction is unavoidable. The load variation of a 450 t passive compensator is typically 2 to 3% roughly equivalent to 100 kN.

3. Active heave compensator sub-system

This is achieved by applying a force onto the load carrying part of the passive compensator to ensure that it cancels out the heave disturbance. The compensating force exerted by the active sub-system as per Newton's 3rd law must consequently react against the heaving vessel.

The active sub-system comprises an actuator, a hydraulic power unit, control system and sensors. The actuator is located at the top of the compensator and the hydraulic power unit (HPU) is typically placed at the base of the derrick which results in long hydraulic lines between the power unit and the actuator; long hydraulic lines are typically associated with transport delays typically 50–90 msec.

This approach uses the pump to metre the flow in either direction directly, that is, to only pump as required and in either direction. This may be achieved by using a swash plate axial piston pump where the swash angle controls the flow; a small servo valve is used to control the pump swash angle using an integral potentiometer. The oil returning from the actuator is delivered to the low pressure side of the pump rather than the tank and this circuit is referred to as closed-loop. This type of hydraulic circuit is inherently more efficient and offers better flow control as it is less affected by back pressure and temperature, but tends to be more expensive and sensitive to contamination (Hatleskog and Dunnigan, 2007a,b; Korde, 1998).

The power capacity of the hydraulic drive and actuator must be sufficient to carry out the compensating task having strict regard to weight and cost issues. An important point to note is that the aim of the active sub-system is to maintain the suspended load stationary with respect to the static environment and thus the oil in the hydraulic lines is the only inertial element to require a power input. The hydraulic drive must have sufficient power capacity at the actuator to overcome the CMC related friction including the viscous friction in the high pressure air lines connecting the CMC to the air bank and the variation in air bank pressure due to the limited air volume. In addition the hydraulic drive must also overcome the viscous friction in the long hydraulic lines to the actuator.

The CMC dynamic performance is typically specified at the nominal maximum operating condition of a 12 foot heave peak-to-peak in a 12 second period which equates to a peak velocity of $1\ \mathrm{m\,s^{-1}}$.

A conventional closed-loop feedback control arrangement would need a relatively high loop gain to reduce the heave disturbance correspondingly; unfortunately the long hydraulic lines with their inherent delays will tend to limit the amount of loop gain that can be applied, thus limiting the performance of this approach. However, as the disturbance, namely the vessel heave, is measurable and the hydraulic drive with sufficient bandwidth, a feed-forward approach may be used to reduce the disturbance. The vessel heave disturbance is measured using a vertical inertial accelerometer; a PD feed-forward controller controls the servo valve of the active drive to push and pull the compensator to match the heave but in the opposite direction, thus cancelling the disturbance. This arrangement as is the feature of all feed-forward arrangements depends on the accuracy of the heave sensor and hydraulic drive to deliver the correct flow at the right time. Any delay in the hydraulic lines will not affect the stability margin of the system but must be countered by a suitable phase advance of the drive signal.

The closed-loop hydraulic drive as illustrated in Fig. 2 is ideally suited for this arrangement as the output flow is directly proportional to the pump swash angle and the feedback loop used to control this is easy to implement with a very good gain margin.

4. Dynamic model

The system dynamic model is described by a set of spring-mass systems which are interlinked as illustrated in Fig. 3 and

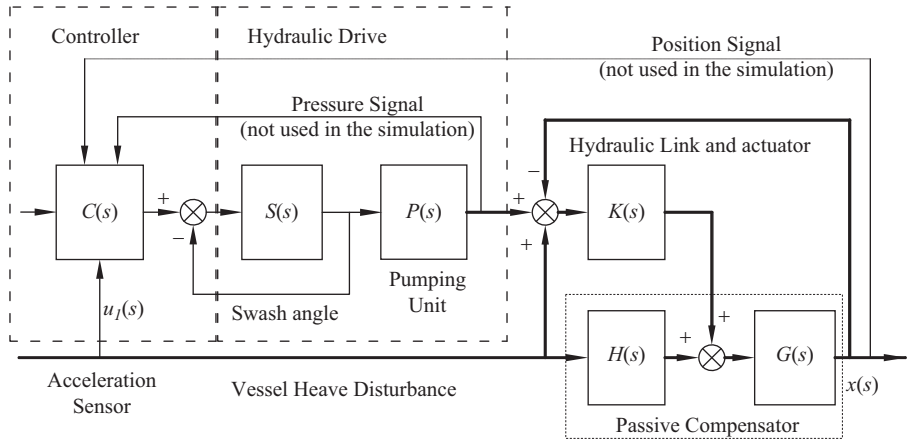

Fig. 2. Detailed System Diagram of Compensator with an active control system.

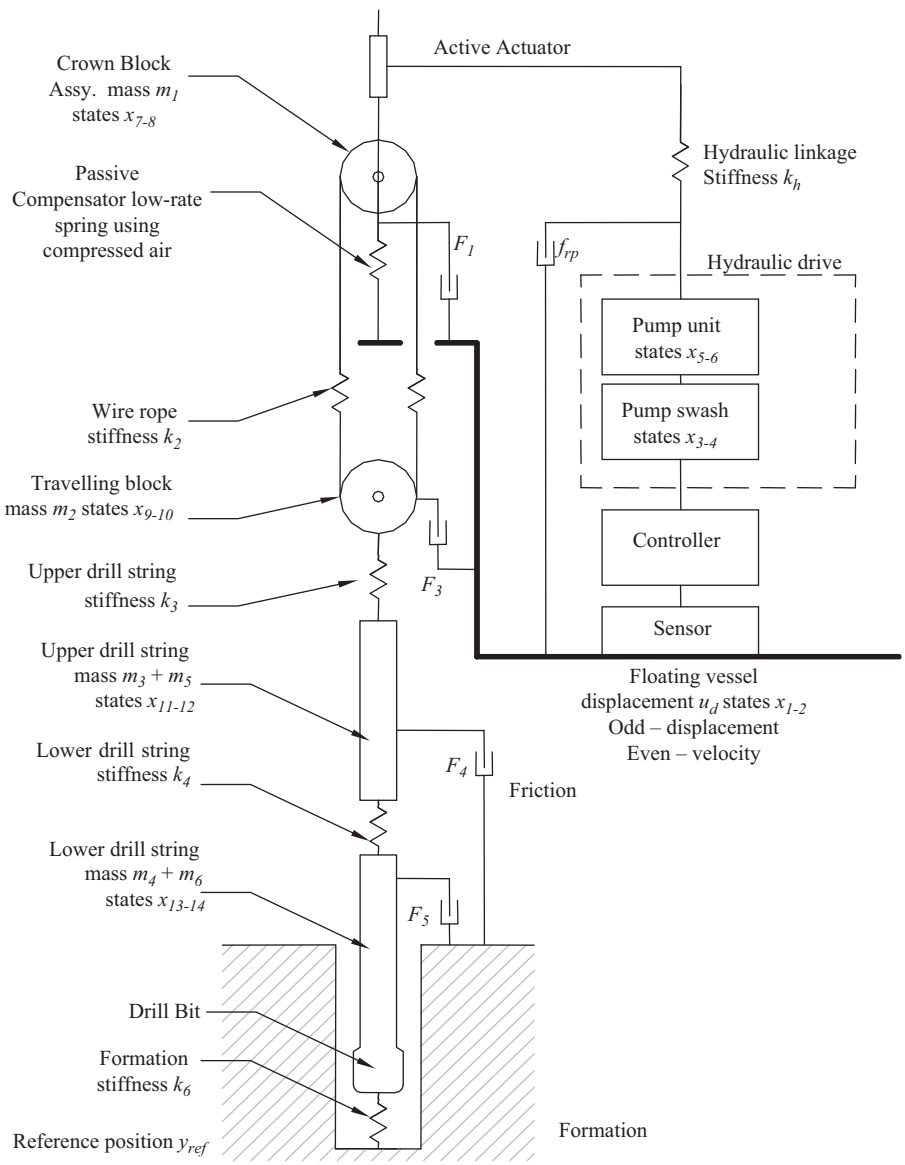

Fig. 3. Dynamic model of the drilling operation with an active compensator.

the resulting second-order differential equations are then transformed into a set of first-order equations and arranged in a solution matrix (1). The compensator dynamic equation is seen to contain two nonlinear elements namely the air spring and the seal friction. In order to ensure a single input in the solution matrix, acceleration is used as the heave disturbance

signal.

$$\begin{bmatrix} \dot{x}_1 \\ \dot{x}_2 \\ \dot{x}_3 \\ \dot{x}_4 \\ \dot{x}_5 \\ \dot{x}_6 \\ \dot{x}_7 \\ \dot{x}_8 \\ \dot{x}_9 \\ \dot{x}_{10} \\ \dot{x}_{11} \\ \dot{x}_{12} \\ \dot{x}_{13} \\ \dot{x}_{14} \end{bmatrix} = \begin{bmatrix} x_2 \\ \ddot{u}_d(t) \\ \frac{k_{s1}\cdot\left[k_{s2}\cdot(k_{s3}\cdot\ddot{u}_d(t)+x_2)-k_{s4}\cdot x_3\right]-fr_s\cdot x_4}{m_s} \\ x_4 \\ x_6 \\ \frac{k_{p1}\cdot x_3-k_{p2}\cdot x_5-fr_p\cdot x_6^2}{m_p} \\ x_8 \\ \frac{k_h\cdot(x_5+x_1-x_7)+p_0\cdot A_1\cdot\left[1-\frac{A_1}{V_0}\cdot(x_1-x_7)\right]^{-k}+sign(x_2-x_8)\cdot F_1-k_2\cdot(x_7-x_9)-m_1\cdot g}{m_1} \\ x_{10} \\ \frac{k_2\cdot(x_7-x_9)-k_3\cdot(x_9-x_{11})+sign(x_2-x_{10})\cdot F_3-m_2\cdot g}{m_2} \\ x_{12} \\ \frac{k_3\cdot(x_9-x_{11})-k_4\cdot(x_{11}-x_{13})+sign(x_{12})\cdot F_4\cdot(x_{12})^2-B\cdot m_3\cdot g}{m_3+m_5} \\ x_{14} \\ \frac{k_4\cdot(x_{11}-x_{13})-\frac{k_6}{2}\cdot((x_{13}-y_{ref})-|x_{13}-y_{ref}|)+sign(x_{14})\cdot F_5\cdot(x_{14})^2-B\cdot m_4\cdot g}{m_4+m_6} \end{bmatrix} \quad (1)$$

The solution matrix comprises of seven second-order DE's each of which requires two state variables; heave disturbance, pump swash, pump and actuator, compensator, travelling block assembly, upper drill sting and the lower drill string section. The modelling of the compensator, travelling block assembly, upper drill string and the lower drill string are described in detail in Hatleskog and Dunnigan, 2007a,b. The variables and constants are listed in the appendix.

The drill bit is in contact with the bottom formation and the formation stiffness k_6 can vary greatly from, for example, soft sandstone which has a bulk modulus of typically 14 GPa and quartz sandstone which is 140 GPa. This can be shown to equate to the stiffness seen by the drill bit as 360 kN m^{-1} on soft formation and 1200 kN m^{-1} on hard formation and 3600 kN m^{-1} on very hard formation.

5. Simulation results

The simulation sea depth is chosen as 1,200 m having drilled to a depth of 1,500 m. The vessel heave is chosen as 1.2 m double amplitude with a 10 s period; this is a condition, which is experienced on a regular basis and also is the limit for some operations. The model is set to apply a mean force at the drill bit against the formation of 60 kN, this is a commonly used 'bit-weight' (Hatleskog, 2008).

The 'balancing pressure' is calculated automatically, but can be modified. Similarly the applied force can be set by adjusting the relative position of the contact surface of the bottom of the well which must also take account of the stretch both in the wire rope and the drill string. These parameters are selected to produce the required bit weight such that the mean applied active actuation is zero. Fig. 4 shows the vessel heave or disturbance and the relative displacement of the compensator, the travelling block and the drill bit which shows that a very good heave reduction can be achieved in terms of displacement using the active sub-system.

The primary measurement used for drilling is the 'weight on bit' or the force applied by the drill bit on the formation it is drilling through. This measure is derived by capturing the total weight suspended from the derrick before contact is made, less the weight when making contact. The load variation is the fluctuation in this measure mainly due to the vessel heave. Fig. 5 shows the load variation at the drill bit when using the active compensation and in this case it is less than 10 kN which can be compared with the corresponding 100 kN load variation of the passive compensator which would be a major improvement.

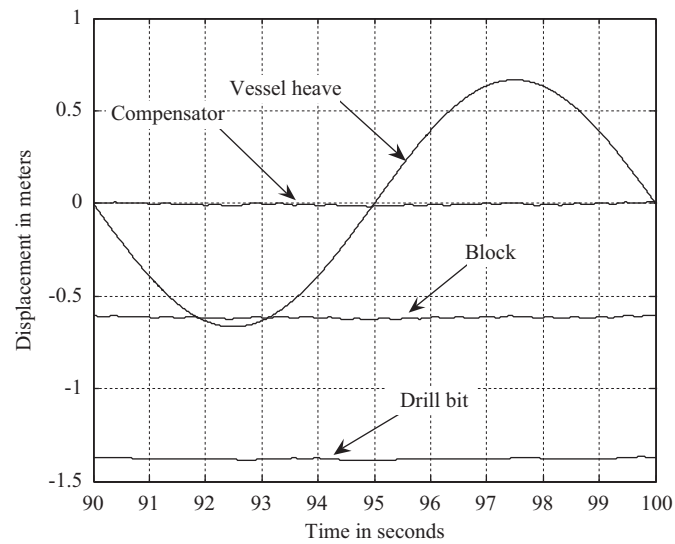

Fig. 4. Heave reduction whilst drilling at 1,200 m on a medium hard formation.

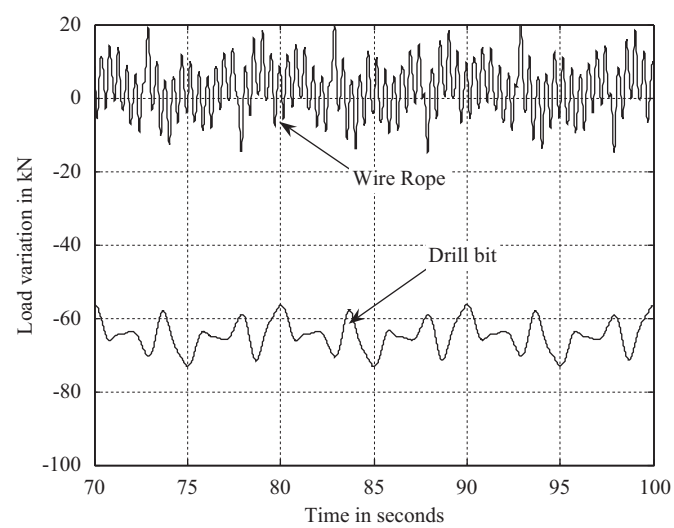

Fig. 5. Load variation drilling at 1,200 m on a medium hard formation.

Also shown is the wire rope load variation which is greater than the variation at the bit and has higher frequency components; this is due to local resonance in the wire rope and corresponds with actual experience. The presence of such rapid fluctuations has tended to deter drillers from using the active compensator system for drilling.

Figs. 6 and 7 illustrate the load variation whilst drilling on soft and very hard formations respectively, showing that the load variation reduces in the case of a softer formation whilst the fluctuations in the wire rope increase marginally.

The sea depth is then set to 100 m having drilled to a depth of 1,500 m which corresponds to parts of the North Sea. Again the vessel heave is chosen as 1.2 m double amplitude with a 10 s period; a mean force at the drill bit against the formation of 60 kN and the same formation sets.

The load variation whilst drilling with the active system at a sea depth of 100 m and on different formation hardness conditions are illustrated in Figs. 8, 9 and 10 and indicate a jerky response on a very hard formation reducing as the formation becomes softer. This is similar to the deepwater case illustrated in Fig. 5. The variation in the wire rope remains similar for the hard

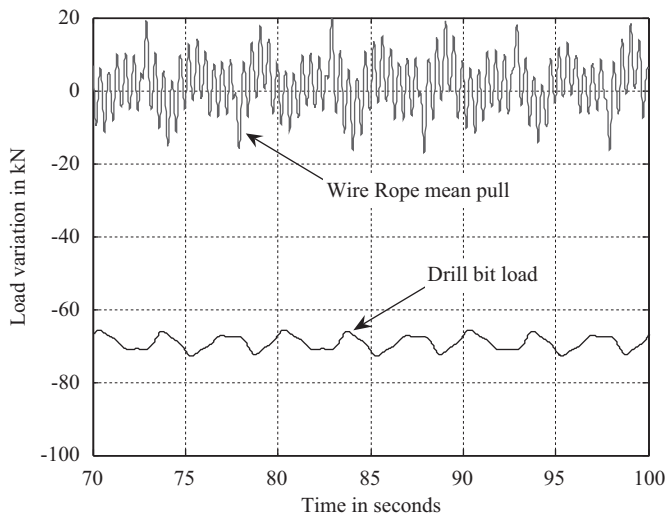

Fig. 6. Load variation drilling at 1,200 m on a soft formation.

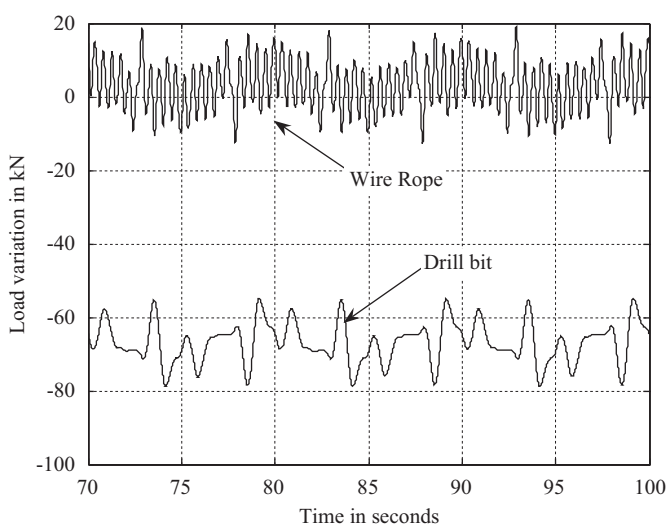

Fig. 7. Load variation drilling at 1,200 m on a hard formation.

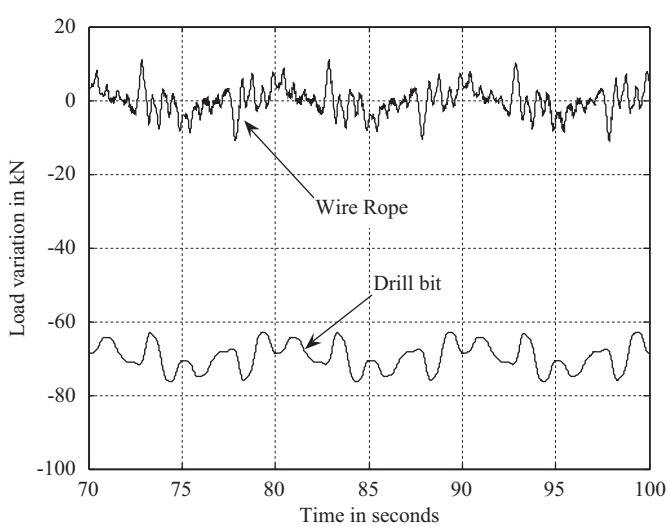

Fig. 8. Load variation drilling at a sea depth of 100 m on a medium hard formation.

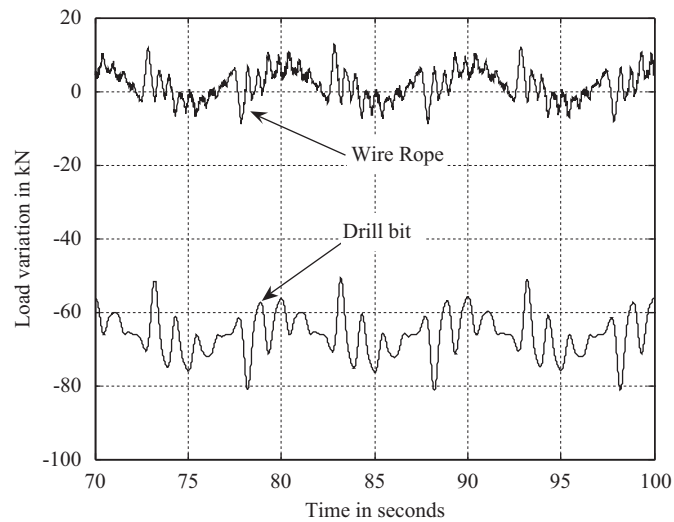

Fig. 9. Load variation drilling at a sea depth of 100 m on a very hard formation.

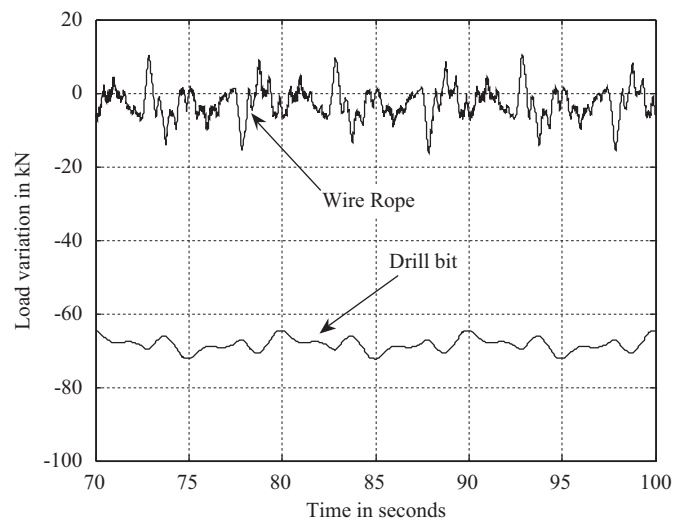

Fig. 10. Load variation drilling at a sea depth of 100 m on a soft formation.

and very hard conditions. In the case of the soft formation the variation in the wire rope appears more erratic but maintains the peak amplitudes as before, although the load variation at the drill bit is much reduced. This type of contact-instability has been experienced in other systems and has been resolved by the use of impedance control techniques.

6. Impedance concept

The concepts of impedance and admittance have been widely used by engineers of different disciplines to generalise and describe many different aspects of interaction between different elements or systems (Bonitz and Hsia T.C., 1996; Colgate and Hogan, 1989; Hogan, 1985; Lawrence, 1988; Whitney, 1977).

The terms impedance and admittance are commonly used to describe sets of two-port networks; it may be a complex term, which may then be described by a vector. In a similar manner, this term may be used for other interacting dynamic systems describing aspects of their interaction such as the relationship between force and displacement. Thus, impedance and admittance may used to describe the interaction of one system and its immediate

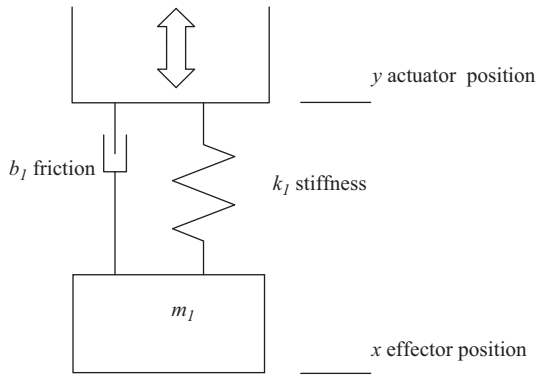

Fig. 11. A second order system.

environment, the term environment in this case is used to denote another system, object, or reference (Glosser and Newman, 1994; Heinrichs and Sepehri, N. 1999).

A mechanical second-order dynamic system, which is attached to an actuator as shown in Fig. 11, may be described by the following expression:

$$m_1 \times \frac{d^2x}{dt^2} + b_1 \times \frac{d(x-y)}{dt} + k_1 \times (x - X_0 - y) + m_1 \times g = 0 \tag{2}$$

Note that X_0 represents the steady-state position, hence $k_1 \cdot X_0 = m_1 \cdot g$ can be used to simplify the transfer function:

$$\frac{x(s)}{y(s)} = \frac{b_1 \times s + k_1}{m_1 \times s^2 + b_1 \times s + k_1} \tag{3}$$

The transfer function (3) illustrates that the steady-state effector position follows the input or actuator position and that any force requirements are directly related to the kinetics of the system.

The effector makes contact with the static environment through a compliant element, which comprises both a stiffness and friction. Such a compliant element may be part of the effector or associated with the static environment.

The transfer function relating the position of the effector to that of the actuator is modified and is shown as expression (4), which includes the additional stiffness and friction elements.

$$\frac{x(s)}{y(s)} = \frac{b_1 \times s + k_1}{m_1 \times s^2 + (b_1 + b_2) \times s + k_1 + k_2} \tag{4}$$

The transfer function (4) illustrates that the steady state position of the effector with respect to the actuator is modified by the stiffness ratio $\frac{k_1}{k_1 + k_2}$.

In addition, the natural frequency of the effector is increased as shown by the expression $\omega_n = \sqrt{\frac{(k_1 + k_2)}{m}}$ and the damping is similarly modified to $\zeta = \frac{(b_1 + b_2)}{2 \times \sqrt{(k_1 + k_2)}}$.

In the case that the stiffness k_2 is relatively high this could lead to a situation with a higher natural frequency and lower damping for the effector. This may explain the difficulty of making light contact by the effector with the environment in the presence of even minor disturbances resulting in instability (Lawrence, 1988; Mason, 1981). This contact-instability might be mitigated by making the actuator apply more force sufficient to ensure a stable contact, but this approach is not appropriate or possible for a wide range of applications and requires other ways of dealing with this problem (Pelletier and Doyon, 1994).

The actuator position may be considered to generate a force, which may be defined as:

$$(m_1 \times s^2 + (b_1 + b_2) \times s + k_1 + k_2) \times x(s) = F(s) \tag{5}$$

Thus, the force may be expressed with respect to displacement as shown:

$$Z(s) = \frac{F(s)}{x(s)} = m_1 \times s^2 + (b_1 + b_2) \times s + k_1 + k_2 \tag{6}$$

The transfer function $Z(s)$ may thus be defined as the generalised impedance of the system. The reciprocal of function of the impedance $Z(s)$ is denoted by the relationships (7) and (8), which is the admittance transfer function of the system.

$$Y(s) = \frac{1}{Z(s)} \tag{7}$$

$$Y(s) = \frac{x(s)}{F(s)} = G(s) = \frac{1}{m_1 \times s^2 + (b_1 + b_2) \times s + k_1 + k_2} \tag{8}$$

In the case that a mechanical sub-system has a mechanical interaction with the object(s) being acted on, mechanical work is exchanged between the mechanical actuator and its environment; the magnitude of the work is a function of the interaction. However, any work or power due to the interaction must relate to the relative angle between the velocity and force vectors.

7. Impedance concept applied to the active compensator

Using active compensation for drilling is a contact operation and gives rise to a degree of contact instability at the drill bit; these rapid fluctuations in the forces experienced by the drill bit are undesirable as they may cause increased wear or damage, particularly on high performance drill bits. In deeper waters the time to change a drill bit is considerable.

In the previous section it was shown that by modifying the impedance structure the contact instability could be avoided by modifying the impedance of the system. In this case the impedance may be altered by adding what is referred to as a 'impedance-sub' between the drill string and the drill bit. It would be precharged to suit the particular drilling conditions. As the drill bit makes contact with the bottom and weight is applied, the impedance sub closes reducing the gas volume thus increasing the pressure and the downward force excerted by the drill bit, just like the compensator.

Fig. 12 illustrates the impedance sub which is connected between the drill bit and the drill string using pin/box screw joints. The stiffness is a function of the change and mean volume of the gas spring. The main source of friction will be the elastomeric seals and to a smaller degree the bearing surfaces. The impedance control approach used to model impedance-sub and drill bit is illustrated in Fig. 13.

As illustrated in Fig. 13 the force transfer function of the impedance sub assembly is:

$$F_{bs}(s) = \frac{k_{bs}}{m_{bs}s^2 + f_{bs}s + k_{bs} + k_6} \tag{9}$$

The natural frequency of the impedance sub assembly is:

$$\omega_{bs} = \sqrt{\frac{k_{bs} + k_6}{m_{bs}}} \tag{10}$$

The very high formation stiffness and the relatively low mass means that the local resonance frequency is relatively high. The drill string sees a relatively low stiffness which can be likened to the earlier soft formation scenario.

Using the differential equation set (1) the impedance sub and drill bit may be added and represented by a second-order differential equation. It is connected to the lower drill string and forms the interface with the formation or static environment. The spring coefficient is determined by the impedance sub configuration and is typically selected as $k_{bs} = 30\ \mathrm{kN\,m^{-1}}$ with the pre-charge set to

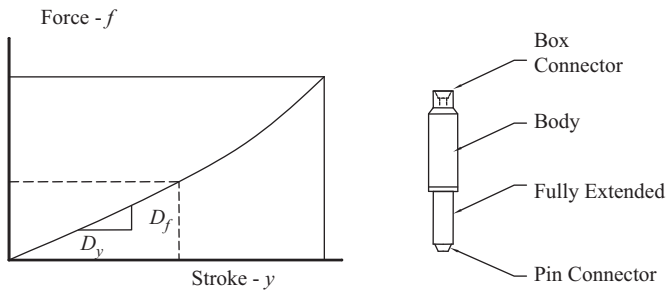

Fig. 12. A typical impedance element illustrating the stiffness or spring coefficient.

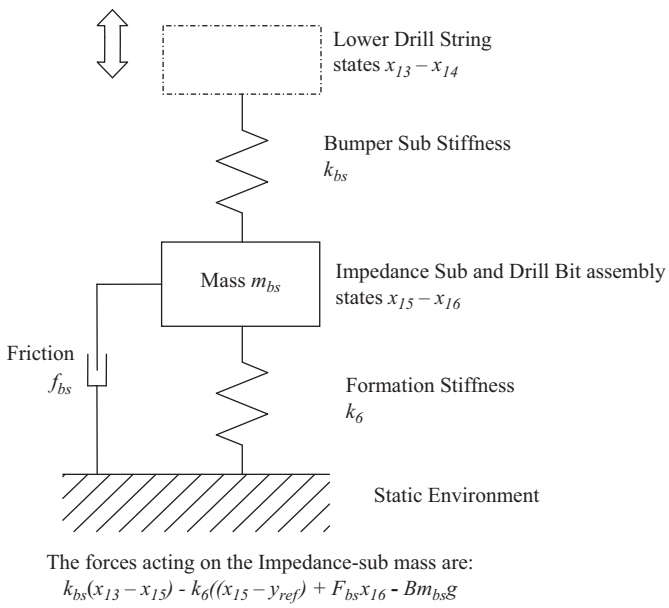

Fig. 13. Dynamic representation of the impedance sub and the drill bit.

provide a downward force of 15 kN in the mid-stroke position. In this case the elastomeric seal friction is relatively high, $F_{bs}=4.5$ kN s m^{-1}. The combined mass of the moving part of the impedance sub and the drill bit is typically $m_{bs}=1{,}200$ kg. In this case a very hard bottom formation with a stiffness of 3600 kN m^{-1} is selected for the simulations as it was previously shown to generate the highest fluctuations.

$$\begin{bmatrix} \dot{x}_1 \\ \dot{x}_2 \\ \dot{x}_3 \\ \dot{x}_4 \\ \dot{x}_5 \\ \dot{x}_6 \\ \dot{x}_7 \\ \dot{x}_8 \\ \dot{x}_9 \\ \dot{x}_{10} \\ \dot{x}_{11} \\ \dot{x}_{12} \\ \dot{x}_{13} \\ \dot{x}_{14} \\ \dot{x}_{15} \\ \dot{x}_{16} \end{bmatrix} = \begin{bmatrix} x_2 \\ \ddot{u}_d(t) \\ x_4 \\ \frac{k_{s1}\cdot\left[k_{s2}\cdot(k_{s3}\cdot\ddot{u}_d(t)+x_2)-k_{s4}\cdot x_3\right]-fr_s\cdot x_4}{m_s} \\ x_6 \\ \frac{k_{p1}\cdot x_3-k_{p2}\cdot x_5-fr_p\cdot x_6{}^2}{m_p} \\ x_8 \\ \frac{k_h\cdot(x_5+x_1-x_7)+p_0\cdot A_1\cdot\left[1-\frac{A_1}{V_0}\cdot(x_1-x_7)\right]^{-k}+sign(x_2-x_8)\cdot F_1-k_2\cdot(x_7-x_9)-m_1\cdot g}{m_1} \\ x_{10} \\ \frac{k_2\cdot(x_7-x_9)-k_3\cdot(x_9-x_{11})+sign(x_2-x_{10})\cdot F_3-m_2\cdot g}{m_2} \\ x_{12} \\ \frac{k_3\cdot(x_9-x_{11})-k_4\cdot(x_{11}-x_{13})+sign(x_{12})\cdot F_4\cdot(x_{12})^2-B\cdot m_3\cdot g}{m_3+m_5} \\ x_{14} \\ \frac{k_4\cdot(x_{11}-x_{13})-k_{bs}\cdot(x_{13}-x_{15})+sign(x_{14})\cdot F_5\cdot(x_{14})^2-B\cdot m_4\cdot g}{m_4+m_6} \\ x_{16} \\ \frac{k_{bs}\cdot(x_{13}-x_{15})-\frac{k_6}{2}\cdot((x_{15}-y_{ref})-|x_{15}-y_{ref}|)+F_{bs}\cdot x_{16}-B\cdot m_{bs}\cdot g}{m_{bs}} \end{bmatrix} \tag{11}$$

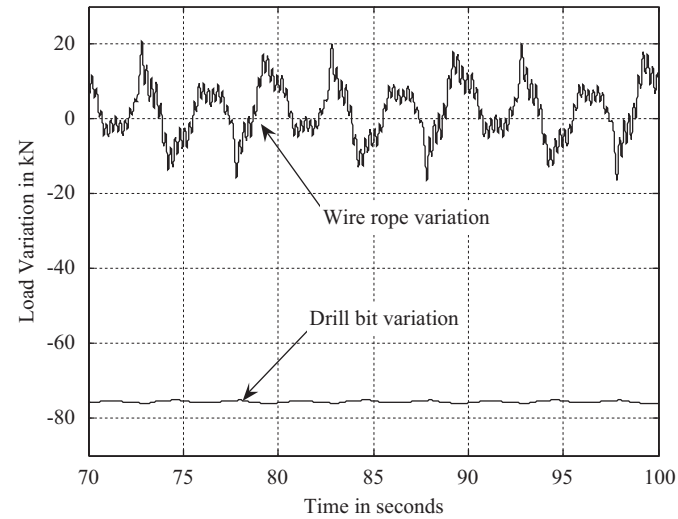

Fig. 14. Load variation drilling at 1,200 m on a hard formation with the Drill Bit Impedance. The variation in the wire rope as excited by the seal friction does not 'reach' the drill bit.

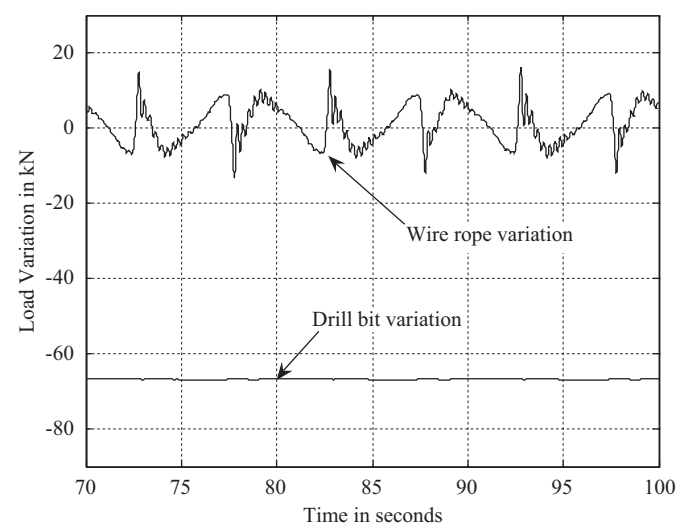

Fig. 15. Load variation drilling at 100 m on a hard formation with the Drill Bit Impedance. The variation in the wire rope as excited by the seal friction does not 'reach' the drill bit.

The complete set of differential Eq. (11) as illustrated by Fig. 3 and 13 is used in the simulations in order to evaluate the load variation both at the drill bit and in the wire rope.

Figs. 14,15 show the load variation using the active system with the impedance-sub added as part of the drill bit, the load variation is greatly reduced at both water depths. This is entirely consistent with the approach modifying impedances as set out by Whitney et. al. circumventing the contact-instability problem by not exciting any local resonances. However, the variation in the wire rope induced by the nonlinear seal friction is still present. It can also be noted that the lower the impedance and variation at the drill bit the higher the variation in the wire rope. This illustrates the difficulty in using the wire rope for measuring the drill bit variation. For a more accurate representation of the actual load variation at the drill bit a different sensing arrangement would be required sensing the load in the drill string.

It can be shown that the wire rope fluctuations are caused by the compensator seal friction simply by changing this nonlinear parameter in the simulation to a linear one. The sharp fluctuation in the wire rope shown in Fig. 14 is seen to relate directly to the

Table A1

List of constants		
		Description
A_1	0.31 m^2	Area compensator cylinder
E_1	60 GPa	Modulus of elasticity wire rope
B	0.777	Buoyancy in drilling fluid
k	1.33	Polytrophic constant
k_h	1.5 10^4 N m^{-1}	Hydraulic linkage stiffness
k_2	3 10^6 N m^{-1}	Stiffness of wire rope
k_3	1.8 10^6 N m^{-1}	Stiffness of drill pipe 1500 m length
k_4	2.3 10^6 N m^{-1}	Stiffness of drill pipe 1200 m length
k_{s1}		Swash loop gain
k_{s2}		Sensor gain
k_{s3}		Acceleration gain
k_{s4}		Scaling factor
fr_s		Swash normalised friction coefficient
m_s		Swash inertial normalised mass
k_{p1}		Pump gain
k_{p2}		Leakage factor
k_6	N m^{-1}	Formation stiffness
k_{bs}	N m^{-1}	Spring coefficient of impedance sub and drill bit assembly
f_{rp}		Swash normalised friction coefficient
m_p		Pump inertial normalised mass
p_0	MPa	System pressure mean
V_0	m^3	Mean system volume

reversal of the compensator stroke and is a function of the non-linear seal coulomb friction.

The rapid fluctuation in the wire rope is due to 'local' resonance; it may be disconcerting but does not reflect the load variation at the drill bit.

8. Conclusion

It has been demonstrated that an impedance strategy can be used to improve the performance of the active compensator by reducing the load variation whilst drilling. The major improvement was achieved by the active system effectively cancelling out the heave disturbance and holding the drill string stationary with respect to the static environment by simply using a proportional controller with a small differential input to provide the required phase advance.

The different impedance control strategies described in this paper were considered for this particular application and it was shown that by using Active Compensator and adding the impedance-sub, thus modifying the impedance shows promise.

Appendix

See Table A1.

References

Bennett, P., 1997. Active heave: The benefits to operations as seen in the North Sea. SPE/IADC 37596, Houston.

Bonitz, R.G., Hsia T.C., T.C., 1996. Internal Force-Based Impedance Control for Cooperating Manipulators. IEEE Trans. Robotics Autom. 12, 78–79.

Colgate, J.E., Hogan, N., 1989. An analysis of contact instability in terms of passive physical equivalents. In: Proceedings of the IEEE International Conference on Robotics and Automation, pp. 404–409.

Glosser, G.D., Newman, W.S., 1994. Implementation of a Natural Admittance Controller on an Industrial Manipulator. In: Proceedings of the IEEE International Conference on Robotics and Automation, pp. 1209–1215.

Hatleskog, J.T., 1983. Drill String Compensators and Riser Tensioning Systems for Offshore Drilling. Trans. Inst. Mar. Eng.0309-394895, 42.

Hatleskog, J.T., Dunnigan, M.W., 2007a. Passive Compensator Load Variation for Deep-Water Drilling. IEEE J. Oceanic Eng. 32 (3), 593–602.

Hatleskog, J.T., Dunnigan, M.W., 2007b. Active Heave Crown Compensation Sub-System. OCEANS 2007—Europe, 1–6.

Hatleskog, J.T., 2008. Modelling and Control of Passive and Active Heave Compensators for Deep Water Drilling. Ph.D. Thesis. Heriot-Watt University, Edinburgh.

Heinrichs, B. and N. Sepehri, N., 1999. A Limitation of Position Based Impedance Control in Static Force Regulation: Theory and Experiment. In: Proceedings of the IEEE International Conference on Robotics and Automation, Detroit Michigan, pp. 2165–2170.

Hogan, N., 1985. Impedance Control: An Approach to Manipulation: Part I—Theory. ASME J. Dyn. Sys., Meas. and Control 107, 1–7.

Korde, U.A., 1998. Active Heave Compensation on Drill-Ships in Irregular Waves. Ocean Eng. 25, 541–561.

Lawrence, D.A., 1988. Impedance Control Stability Properties in Common Implementations. IEEE Conf. Robotics and Automation. April, vol. 2, pp. 1185–1190.

Mason, M.T., 1981. Compliance and Force Control for Computer-Controlled Mechanical sub-systems. IEEE Trans. Syst., Man, Cybern., SMC 11 (6), 418–432.

Pelletier, M., Doyon, M., 1994. On the Implementation of Impedance Control on Position Controlled Robots. In: Proceedings of the IEEE, vol. 2. pp. 1228–1233.

Whitney, D.E., 1977. Force Feedback Control of Manipulator Fine Motion. ASME J. Dyn. Syst., Meas. Control, 91–97.

Woodall-Mason, N., Tilbe, J.R., 1976. Value of heave compensators to floating drilling. J. Pet. Technol., 938–942.